Title

Mechanobactericidal Nanotopography on Nitrile Surfaces toward Antimicrobial Protective Gear

Journal

ACS Macro Letters, 12(2)

ISSN

2161-1653

Authors

Patil, Deepak
Golia, Vibhanshu
Overland, Maya
et al.

Publication Date

2023-02-21

DOI

10.1021/acsmacrolett.2c00697

Peer reviewed

ACS Macro Letters

pubs.acs.org/macroletters Letter

Mechanobactericidal Nanotopography on Nitrile Surfaces toward Antimicrobial Protective Gear

Deepak Patil, Vibhanshu Golia, Maya Overland, Marshall Stoller, and Kaushik Chatterjee*

Cite This: *ACS Macro Lett.* 2023, 12, 227−233 Read Online

ACCESS | Metrics & More | Article Recommendations | Supporting Information

ABSTRACT: We have much to learn from other living organisms when it comes to engineering strategies to combat bacterial infections. This study describes the fabrication of cicada wing-inspired nanotopography on commercially pure (CP) nitrile sheets and nitrile gloves for medical use using the reactive ion etching (RIE) technique. Antibacterial activity against *P. aeruginosa* was tested using two different surface morphologies. It was observed that the etched nitrile surfaces effectively minimized bacterial colonization by inducing membrane damage. Our findings demonstrate a single-step dry etching method for creating mechanobactericidal topographies on nitrile-based surfaces. These findings have utility in designing next-generation personal protective gear in the clinical setting and for many other important applications in the age of antimicrobial resistance.

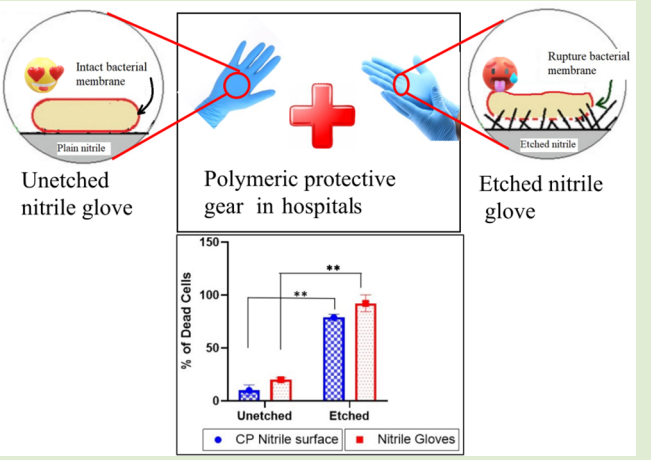

The development of novel antimicrobial surfaces that can combat microbial contamination and minimize the spread of infection has been gaining increased attention.[1] Contaminated biomedical implants, surgical tools, hospital furniture, personal protective gear, and other clinical surfaces are all potential sources of hospital-acquired infections (HAIs).[2] It is now well recognized that microorganisms have evolved biochemical and mechanical strategies, including biofilm formation and the emergence of multidrug resistance (MDR) to overcome standard antibacterial approaches.[3,4] This, in turn, makes HAIs increasingly difficult to treat, often requiring prolonged intravenous systemic antibiotic therapy, sometimes with multiple agents. Therefore, there is a pressing need for novel strategies to be developed to suppress MDR microbial contamination and spread on clinical surfaces.

In contrast to antibiotics, which have a biochemical mechanism of action, nanomaterials can leverage distinct physical mechanisms against bacteria. The identification of the mechanobactericidal response of nanotopography present on insect (e.g., cicada and dragonfly) wings in the past decade has motivated the fabrication of nanostructured topography on synthetic materials to minimize bacterial colonization of the surfaces.[5] Most of the reported studies in the scientific literature focused on hard materials such as silicon and metallic materials such as titanium and aluminum alloys. Recently, lethal damage and physiological changes to bacteria that are adhered to high-aspect-ratio nanostructured surfaces have been revealed.[6−8] Membrane cutting or stretching mechanisms are identified and caused by two categories of forces: (i) pressure exerted by the sharp nanostructures[9,10] and (ii) tension forces induced by the energy stored and released during the deformation of flexible nanostructures.[11]

Flexible, softer surfaces, such as polymers and composites, are widely used for medical and food packaging, the textile industry, and wearable electronics and are equally prone to bacterial contamination. However, there is limited research on mechanobactericidal nanostructures on polymeric materials. Recently, Ivanova et al. fabricated 60 nm structures on poly(ethylene terephthalate) and polypropylene to demonstrate antibiofouling properties for food packaging applications.[6] However, polymers such as nitrile, commonly used for surgical gloves and aprons in healthcare applications, have yet to be investigated.

Standard micro- and nanofabrication processes, such as nanoimprint lithography and a hybrid of colloidal lithography and plasma etching, are multistep, slow, and limited to thermoplastics.[12] In contrast, reactive ion etching (RIE) is a one-step simple and elegant procedure that can generate random nanotopography on a wide range of materials.[13]

Received: November 27, 2022
Accepted: January 19, 2023
Published: January 27, 2023

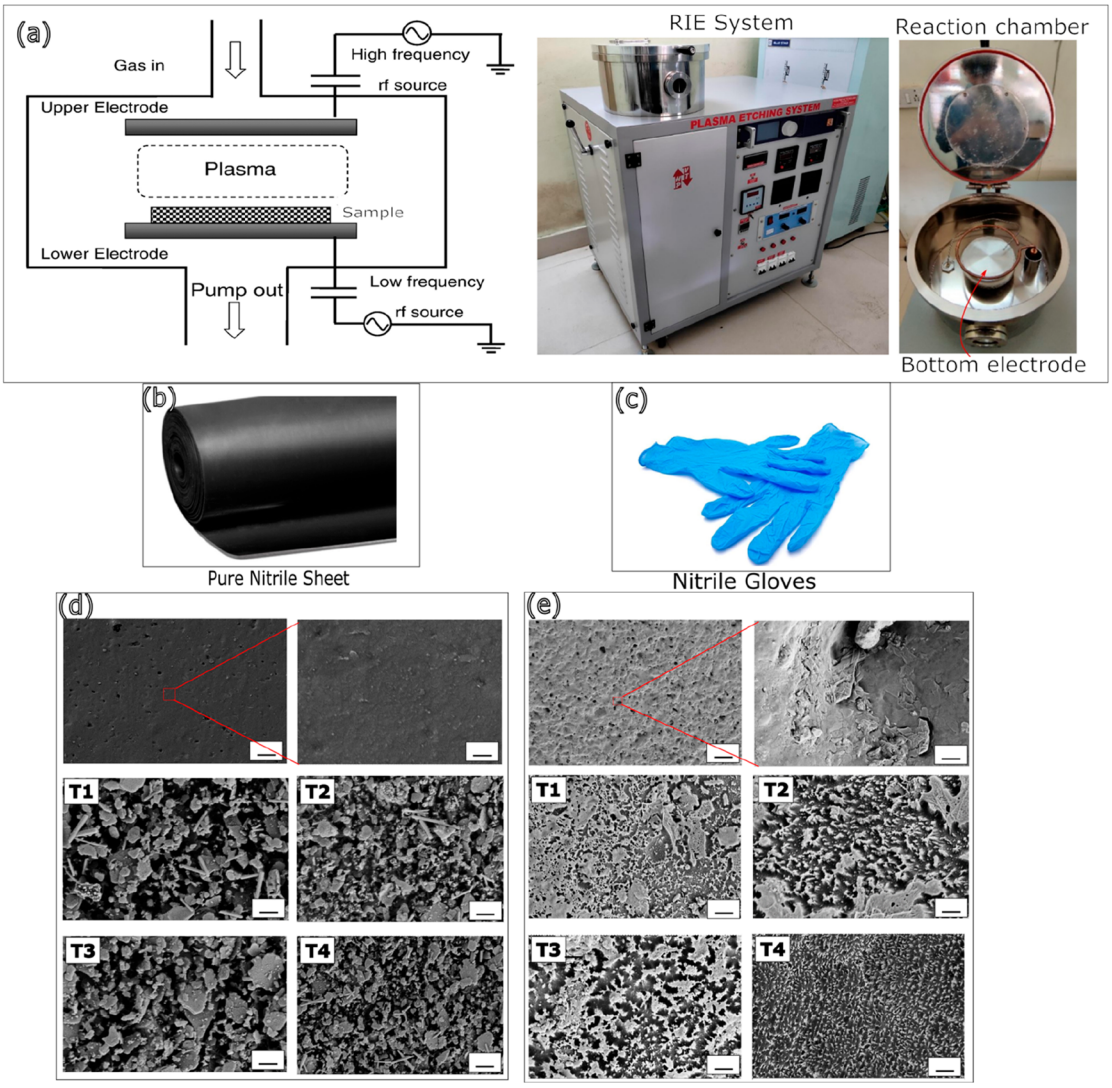

Figure 1. (a) Schematic of the RIE chamber and photograph of RIE system and reaction chamber (interior view) used in this study; (b, c) Photographs of CP nitrile sheet and medical grade nitrile gloves; (d, e) FESEM micrographs of nanostructures generated on (d) a CP nitrile sheet; (e) Nitrile gloves using various recipes described in Table 1. Scale bars are 1 μm.

However, the applicability of this manufacturing process to engineer mechanobactericidal nanostructures on polymers for medical products and protective gear has not been demonstrated before.

Nitrile gloves worn during medical examinations and procedures are widely used as disposable personal protective gear. When compared to latex, natural rubber, or vinyl gloves, these are lightweight, have an extended life, and have a superior puncture and chemical resistance.[14] Nitriles find utility in a range of applications, including medical devices, food packaging, external protection, and high-voltage line insulators.[14] Bacteria can adhere to nitrile surfaces leading to the spread of infections, which is of particular concern in the clinic and food industry and underscores the need to engineer antibacterial nitrile surfaces. The goal of this study was to fabricate and test bactericidal nanostructures on commercially pure (CP) nitrile surfaces by RIE and extend this to commercially sourced medical-grade nitrile gloves.

Flat nitrile substrates (CP nitrile sheet and gloves) were subjected to dry etching using O_2 plasma inside a custom-built RIE chamber in a capacitively coupled configuration. Figure 1a presents the schematic design of a custom-built RIE system along with a photograph of the RIE system with an interior view of the reaction chamber. The system consists of a reaction chamber with two electrodes where a gas or a combination of gases are introduced at low pressures and temperatures. The sample is placed on the lower electrode connected to a 13.56 MHz radio frequency (RF) power supply. Gases are introduced through a showerhead at the top of the chamber and subsequently ionized by the bias applied to the lower electrode (cathode).[15] The pressure inside the chamber is maintained with the help of a vacuum pump circuit consisting of a turbomolecular pump backed by a rotary pump. In this system, gas compositions and flow rate, RF power, chamber pressure, and substrate temperature influence the etching process and are key parameters in determining the resultant topography.[16] Thus, a range of values of these parameters was studied, holding substrate temperature at 20 °C, and gas composition was fixed as pure oxygen (see the Supporting Information file for additional details). Figure 1b,c shows photographs of the CP nitrile sheet and nitrile gloves from which the smaller samples were cut for RIE. Generation of

https://doi.org/10.1021/acsmacrolett.2c00697
ACS Macro Lett. 2023, 12, 227−233

nanostructures via RIE involves physical sputtering of the surface by incoming ions as well as chemical reactions between the plasma species and the substrate surface. Plasmas are mostly produced by a high-frequency discharge, which causes higher acceleration of electrons due to their lower mass, while heavier ions are only slightly affected, resulting in greater dissociation of the feeding gas. Highly dissociated plasmas are produced by inductively coupled RF discharges. When neutral radicals interact with a surface, potential energy interactions are more important than kinetic energy interactions. To react with an exposed surface, a plasma particle must have enough energy to overcome the activation energy barrier for a chemical reaction. Thus, the energy of the particles generated in the system can be used to control the etching rate in plasma. This can be altered by adjusting discharge parameters such as plasma or RF power, gas flow rate, and chamber pressure.[17] A range of values of the three process parameters, namely chamber pressure, gas flow rate, and RF power, were tested to identify parameters that can yield uniform nanostructures. The combination of process parameters used for etching is listed in Table 1.

Table 1. Combination of Process Parameters Used in RIE

surface topography notation	RF power (W)	gas flow rate (sccm)	chamber pressure (mbar)
T1	30	20	0.05
T2	60	20	0.05
T3	30	50	0.05
T4	60	50	0.05

The formation of random nanoscale features is ascribed to preferential etching by oxygen plasma directed by the codeposition of metallic nanoparticles randomly sputtered from the cathode.[18] Such metal codeposition results in the formation of micromasks on the polymer surface, and the area directly beneath such masks have a slower etch rate than the pristine regions of nitrile. This process of micromasking is reminiscent of the generation of nanostructures on surfaces.[13] The nanoscale structures similar to those found on insect wings were formed on the nitrile substrates with all of the recipes listed in Table 1, although the characteristic features of the nanoarchitectures were different.

Alterations in the working parameters of the chamber affect the etching rate, thereby changing the energy of the particles. Momentum transfer from the incident ion is associated with the physical etching of the substrate. RF power controls this momentum. The etch rate increased with an increase in the chamber pressure. As the pressure is increased, the availability and density of reactive species in the chamber also increase, thereby increasing the etching rate. This also results in a decrease in anisotropy of etching due to the reduced mean free path of the ions, which causes more frequent collision events and deviation of the ions from their original straight path and an increase in their angular distribution.[13] However, in this study, chamber pressure (0.05 mbar) was kept constant. The gas flow rate determines the availability of fresh reactive species in the chamber for chemical etching and, therefore, decides the etch rate. Greater availability of reactive species means a higher etch rate. Lowering the power (T1), which controls the dissociation percentage of the incoming gas (plasma density) and the kinetic energy of the ions, resulted in insufficient etching of the surface, whereas increasing the power (60 W) resulted in complete etching with uniform nanostructures throughout the surface (Figure 1e, T4). A low gas flow rate (20 sccm, T1) is inefficient for etching the entire surface, resulting in pits and holes (Figure 1e), whereas increasing the gas flow rate (which determines ion residence time) increases etching isotropy. The nanostructures formed at 50 sccm O_2 flow rate closely resembled nanostructures found on cicada wings.[5] In the case of the CP nitrile sheet, the etched surface looked nearly similar in all four conditions (T1−T4), whereas nitrile gloves had distinct nanotopographies.

A mask or mold with the desired dimensions of the target nanostructures is an essential first step. One of the techniques makes use of a commercially available anode aluminum oxide (AAO) template as a mask.[6,24] The plasma interacts with the substrate via the nanoscale opening of the AAO template and etches out the substrate. The nonexposed area transforms into insect-inspired nanopillars that remain on the substrate.[24] The polymer can be molded in the AAO template's nano-opening and replicated as nanoprojections on polymer surfaces.[6] Nanospheres can also be used as masks on a polymer substrate, with the exposed area between the nanospheres etched away by RIE.[25] Nanostructures resembling those on cicada wings can also be realized using hot embossing and UV nanoimprinting techniques.[26]

However, these aforementioned processes require a mask or mold to cover a small area each time.[27] The polymers must be molded in a mold for the nanoimprint and hot embossing processes, limiting these two techniques to thermoplastics. Notably, the above-mentioned processes are limited to flat surfaces due to the use of masks/molds, whereas maskless RIE can easily be applied to curved surfaces. The random nanostructures generated by RIE have demonstrated excellent mechanobactericidal activity against several strains of bacteria along with the added advantage of cost-effective scalability.[13,28,29] In contrast to periodic structures, the random nanostructures are more densely packed, and owing to their random arrangements, the bacteria are exposed in many different directions to the pillar tips.[13,29]

Fourier transform infrared (FTIR) spectroscopy was used to investigate the chemical composition of the substrates and determine potential changes induced by exposure to plasma etching (see Figure S1). The results demonstrate that the dry etching process did not affect the chemical characteristics of the samples. No additional peaks or attenuation of peaks present prior to etching were noticed in the etched CP nitrile and on nitrile gloves after etching. Notably, the FTIR spectra reveal differences in the chemical characteristics between the CP nitrile sheets and the nitrile gloves, which could be attributed to the distinct compositions used to manufacture gloves. XPS analysis revealed no significant differences in chemical composition between etched and unetched surfaces (see Figure S2). The nitrile gloves have additional elements such as Si, Cl, and Zn, which are used as additives for manufacturing gloves. Their atomic fractions can be seen in Table S1. Nitrile gloves are made from Nitrile Butadiene Rubber (NBR), a synthetic material created in a large vat by combining monomers such as butadiene and acrylonitrile, which polymerize to result in liquid nitrile. The nitrile is then filtered and combined with antioxidant and coagulating agents by glove manufacturers to create a more durable material.[14] This study focused on CP nitrile sheets procured from only one manufacturer. However, the variety of additives used by different manufacturers while making nitrile gloves could affect

https://doi.org/10.1021/acsmacrolett.2c00697
ACS Macro Lett. 2023, 12, 227−233

the ability to create nanostructures using RIE. The evidence for this can be seen from the formation of different nano topography on CP nitrile sheet and nitrile glove, which has additional additives to make manufacturability easy. Each element uniquely influences the etching rate and the topography generated. Sometimes, these gloves are coated or chlorinated for ease of wearing and removal, which may also influence the nanotopography.[14] The process parameters may be optimized for preparing gloves with mechanobactericidal nanostructures.

For the nitrile gloves, uniform etching was observed for conditions T3 and T4. Hence, these two conditions were further investigated for detailed surface characterization and evaluation of antimicrobial activity using colony forming assay and Alamar Blue assay (see SI for detailed methodology). Table 2 compiles the arithmetic average roughness (R_a) and the height of the maximum profile wave crest (R_p) values of the unetched and etched surfaces for various recipes. Figure 2a–d shows the corresponding optical micrographs. The etched surfaces are rougher than the unetched surface, which can influence surface wettability and bacterial attachment. Surface roughness has been shown to increase the adhesion force of bacterial cells at specific points, which may result in cell damage.[5] The surface wettability of the nitrile surfaces was determined using static water contact angle measurements.

Table 2. Roughness Values of Selected Etched Surfaces

	R_a (μm)		R_p (μm)	
conditions	CP nitrile sheet	nitrile gloves	CP nitrile	nitrile gloves
unetched surfaces	0.2016	0.4477	0.3251	0.8705
T3	1.021	1.121	0.9210	1.001
T4	1.321	1.400	1.281	1.422

The static water contact angle on the nanostructured CP nitrile surface decreased to 7.5 ± 1° from 82 ± 2° after etching, whereas the contact angle on the nanostructured glove decreased to 12 ± 1° from 78 ± 2° for the gloves (Figure 2e). This increased water wettability is attributed to an increase in the total surface area caused by nanostructures, resulting in a transition from Young's to Wenzel's state of wetting. Another contributing effect is the change in surface composition and the presence of O-rich functional group on the etched surface, imparting surface polarity.[23]

To evaluate the mechanobactericidal activity against Gram-negative *P. aeruginosa*, etched T3 and T4 topographies were tested and compared with the unetched surface. We used the colony count method to assess the antibacterial activity of all three surfaces, following a modified ISO standard (International Organization for Standardization) JIS Z 2801 protocol for assessing the contact-killing antibacterial efficacy of nitrile surfaces.[19] Figure 3a shows representative photographs of colonies formed in Petri dishes retrieved from the surfaces of the etched nitrile gloves. After 24 h of incubation, unetched substrates had a higher bacterial colony count, indicating that bacteria could survive and thrive on these surfaces (Figure 3b). In contrast, for both T3 and T4 conditions, the bacterial counts were much lower on both the etched CP nitrile sheet and the glove surface. To validate the colony count, bacterial growth on unetched and etched surfaces was measured with the Alamar Blue assay. The absorbance values are plotted in Figure 3c. The absorbance value denotes metabolically active cells and is indicative of the number of viable cells. The fluorescence intensity is remarkably lower on the etched surfaces for both T3 and T4 conditions, corroborating the trends seen in CFU.

Furthermore, the T4 surface appears to have significantly better antibacterial performance than the T3 surface. This difference is likely because the surface nanostructures for T4 are very uniformly distributed on the etched nitrile gloves (Figure 1e). SEM was used to examine the morphology of bacterial cells attached to the unetched and nanostructured nitrile (T4) surfaces. The cells were intact and adhered well on the unetched surfaces (Figure 4a,b), whereas the micrographs revealed clear damage to the bacterial cell wall on T4 (Figure 4d,e), confirming that the surface nanostructures damaged the cell wall and caused bacterial death. Furthermore, confocal micrographs showed that the nanotopographies were highly bactericidal when compared to the unetched nitrile surfaces, where the majority of the cells were viable (Figures 4c,f and S3).

On a flat surface, the bacterial surface proteins on the contact area tether to the surface, resulting in strong adhesion, and adhesion decreases as the contact area is reduced on the

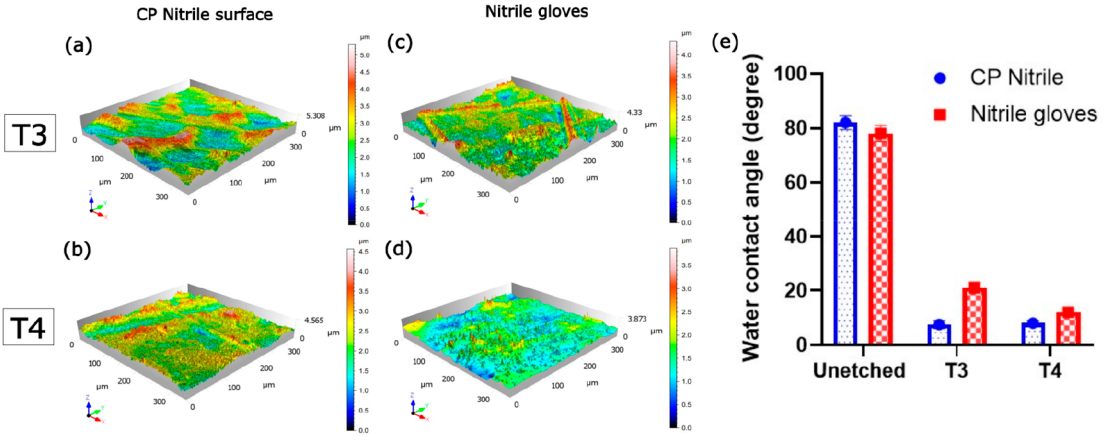

Figure 2. Optical profilometry micrographs for recipes T3 and T4 for the etched surface. (a, b) 3D surface pattern for CP nitrile surface and (c, d) nitrile gloves. (e) Water contact angle values as measured on unetched and T3 and T4 surfaces. Surfaces became hydrophilic after the generation of nanostructures, possibly due to the formation of a Wenzel state.

https://doi.org/10.1021/acsmacrolett.2c00697
ACS Macro Lett. 2023, 12, 227–233

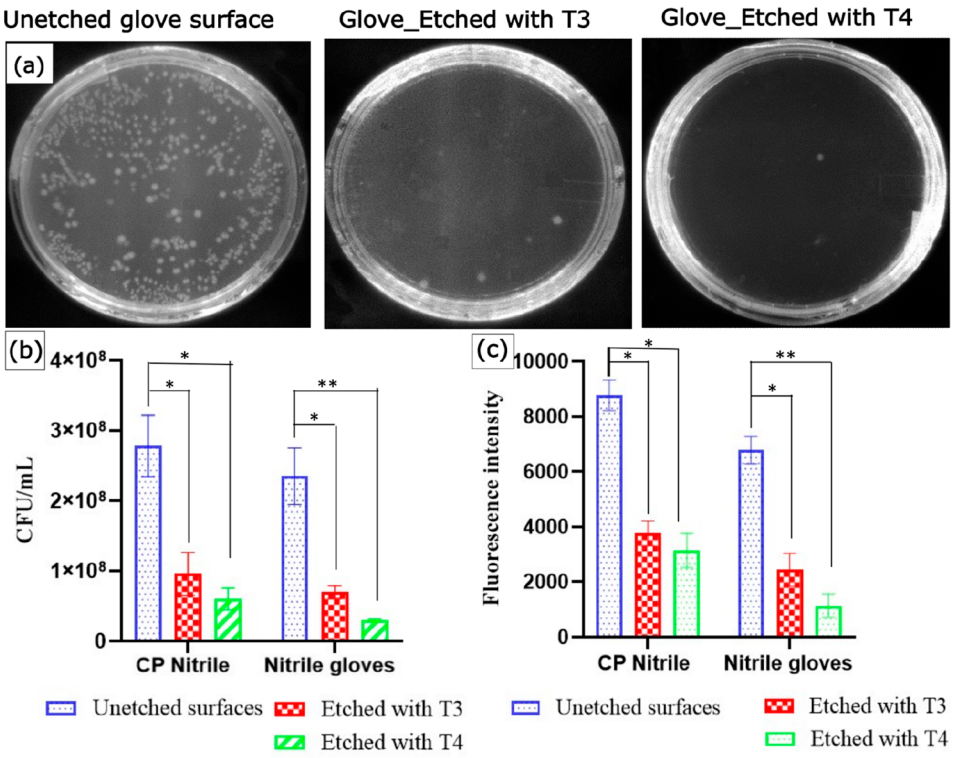

Figure 3. (a) Representative photographs of colonies formed in a Petri dish retrieved from etched nitrile gloves with reference to the unetched surface. (b) The bar graph represents the bacterial colony count retrieved from different samples after 24 h, (c) The fluorescence intensity from the Alamar Blue assay represents the relatively metabolically active bacterial cells on the surfaces. * indicates significance for $p < 0.05$ and ** indicates $p < 0.01$ (one-way ANOVA). The data are presented as mean ± SD for $n = 3$.

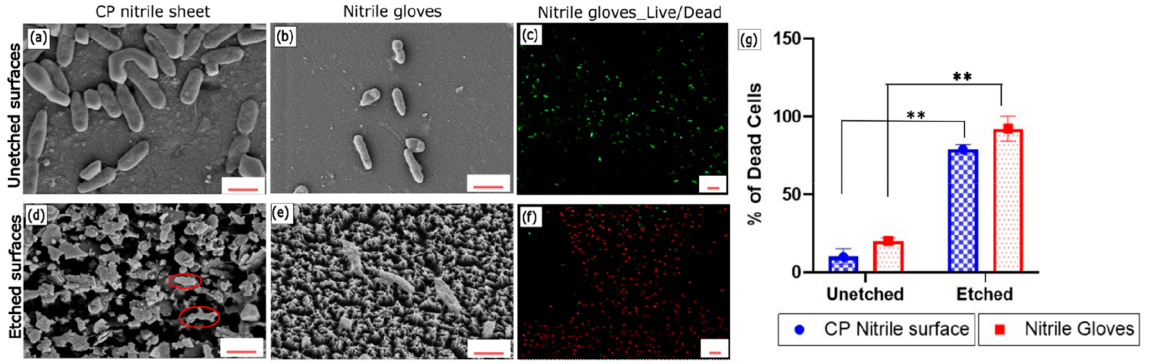

Figure 4. Qualitative observation of mechanobactericidal performance of the etched nanostructured nitrile surfaces with respect to the unetched surfaces. (a, b) SEM micrographs show intact *P. aeruginosa* on unetched surfaces (d, e) SEM micrographs show the cell wall deformation on the nanostructured topographies. Scale bar 1 μm (c, f) Representative Live/Dead confocal micrographs of *P. aeruginosa* for unetched and etched nitrile gloves (60×) and (g) bar graph showing the percentage of dead cells on unetched and nanostructured samples. ** indicates significance for $p < 0.01$ (one-way ANOVA). The data are presented as mean ± SD for $n = 3$.

etched surfaces. Furthermore, as the height of the asperities increases, it becomes increasingly difficult for the bacteria to reach the substrate floor between the nanostructures, preventing them from attaching. The antibacterial efficacy was quantified via direct counting of nonviable appearing cells from the confocal micrographs, and more than 85% of the cells were found dead on the nanostructured surfaces. The observed bacterial killing property arises from the nanostructures, which is consistent with the previously reported data on other kinds of surfaces, such as insect wings as well as black silicon and black titanium.[5,20] Despite differences in the surface composition of the CP nitrile sheet and gloves, the etched surface exhibited excellent bactericidal activity on both substrates, demonstrating that the antibacterial phenomenon can be attributed to the nanoscale roughened surface as a result of etching. Other studies have demonstrated the topography-mediated bactericidal activity of cicada wings, dragonfly wings, and black silicon using a similar strategy of coating with nonbactericidal gold.[10,20,21] Although there are many models proposed to elucidate the mechanobactericidal activity of nanostructured surfaces, the two prominent mechanisms underlying cell-topography interactions include (i) rupture of bacterial membrane suspended between two nanostructures[30] and (ii) membrane rupture at the tip of nanostructures.[31,32] In

https://doi.org/10.1021/acsmacrolett.2c00697
ACS Macro Lett. 2023, 12, 227−233

the first mechanism, the stretching of the bacterial cell membrane beyond its elastic limit results in membrane rupture in the regions suspended between nanopillars as the cell adsorbs onto the nanostructured surface.[30] However, subsequent studies suggested that the tips of nanostructures would rupture.[31] In the second mechanism, the bacterial membrane ruptures when the maximum stress at the interface of the nanostructure tip and the membrane exceeds the local maximum allowable membrane strain.[32] The second mechanism may be used to explain the mechanobactericidal property of the etched nitrile surface. SEM images show that *P. auregenosa* cells become deformed and eventually punctured at the tips of the nanostructures.

Notably, variations in the composition and morphology of the membrane among different strains affect the killing efficacy. Membrane integrity of a bacterium is maintained by an internal turgor pressure in conjunction with the peptidoglycan layer. The difference in peptidoglycan layer thickness between Gram-negative (thin peptidoglycan layer) and Gram-positive (thick peptidoglycan layer) bacteria induces changes in turgor pressures and their ability to resist mechanical stress generated by the nanostructures.[33] Adsorption of the cell membrane onto nanofeatures stresses the cell wall, thereby increasing the turgor pressure and stiffening of the cell wall.[30,34] Therefore, cell wall rigidity and other micromechanical properties of a cell are the main aspects that affect the susceptibility of bacteria to the mechanobactericidal action of nanostructured surfaces.[35−37] Furthermore, it has been simulated that bacteria-nanostructures depend on cell properties such as bacterial stretching modulus, bending modulus, and cell membrane adhesion energy, which differ between bacteria.[34] Hence, all the above parameters could affect the bactericidal efficacy of different bacteria interacting with a given nanostructured surface.

In summary, bioinspired mechanobactercidal structures were fabricated on CP nitrile surfaces and commercially supplied nitrile gloves using the RIE technique. For nitrile glove surfaces, the optimal combination of process parameters was discovered to produce uniform nanostructures throughout the surface, whereas the same combination produces different surface textures on pure nitrile sheets. Analogously, when different aluminum alloy compositions were etched using hydrothermal treatment, varying surface topography was observed.[22] The RIE method described in this study offers a one-step effective process to create mechanobactericidal structures on nitrile-based surfaces, offering a promising mechanical approach to halting the surface spread of bacteria in clinical and other settings.

■ ASSOCIATED CONTENT

Supporting Information

The Supporting Information is available free of charge at https://pubs.acs.org/doi/10.1021/acsmacrolett.2c00697.

Detailed experimental methods; FTIR and XPS spectra of the unetched and etched nitrile surfaces; atomic fractions determined from XPS; Fluorescent micrographs of bacterial cells on the surfaces; Summary of the typical production of nitrile gloves (PDF)

■ AUTHOR INFORMATION

Corresponding Author

Kaushik Chatterjee − *Department of Materials Engineering, Indian Institute of Science, Bengaluru 560012, India;* orcid.org/0000-0002-7204-2926; Phone: +91-80-22933408; Email: kchatterjee@iisc.ac.in

Authors

Deepak Patil − *Department of Materials Engineering, Indian Institute of Science, Bengaluru 560012, India*

Vibhanshu Golia − *Department of Materials Engineering, Indian Institute of Science, Bengaluru 560012, India*

Maya Overland − *Division of Pediatric Urology, Children's Hospital of Philadelphia, Philadelphia, Pennsylvania 19104, United States*

Marshall Stoller − *Department of Urology, University of California, San Francisco, California 94143, United States*

Complete contact information is available at: https://pubs.acs.org/10.1021/acsmacrolett.2c00697

Author Contributions

CRediT: **Deepak Patil** conceptualization (equal), data curation (lead), formal analysis (lead), investigation (equal), methodology (lead), writing-original draft (lead); **Vibhanshu Golia** data curation (supporting), formal analysis (supporting), investigation (supporting), methodology (supporting), writing-original draft (supporting); **Maya Overland** conceptualization (supporting), methodology (supporting), project administration (supporting), supervision (supporting), writing-review & editing (supporting); **Marshall Stoller** funding acquisition (equal), project administration (supporting), supervision (supporting), writing-review & editing (supporting); **Kaushik Chatterjee** conceptualization (equal), formal analysis (supporting), funding acquisition (lead), methodology (equal), project administration (lead), supervision (lead), writing-review & editing (lead).

Notes

The authors declare no competing financial interest.

■ ACKNOWLEDGMENTS

The authors gratefully acknowledge the Department of Science and Technology (DST), Government of India (Project DST/AISRF/2020/54) and UCSF for funding. The authors would like to thank Mr. Anindo Roy for his help and fruitful discussions about etching nitrile surfaces with the customised RIE system.

■ REFERENCES

(1) Balasubramaniam, B.; Prateek, P.; Ranjan, S.; Saraf, M.; Kar, P.; Singh, S. P.; Thakur, V. K.; Singh, A.; Gupta, A. K. Antibacterial and Antiviral Functional Materials: Chemistry and Biological Activity toward Tackling COVID-19-like Pandemics. *ACS Pharmacol. Transl. Sci.* **2021**, *4* (1), 8−54.

(2) Donlan, R. M. Biofilms and Device-Associated Infections. *Emerg. Infect. Dis.* **2001**, *7* (2), 277−281.

(3) Catalano, A.; Iacopetta, D.; Ceramella, J.; Scumaci, D.; Giuzio, F.; Saturnino, C.; Aquaro, S.; Rosano, C.; Sinicropi, M. S. Multidrug Resistance (MDR): A Widespread Phenomenon in Pharmacological Therapies. *Molecules* **2022**, *27* (3), 616.

(4) Olar, R.; Badea, M.; Chifiriuc, M. C. Metal Complexes—A Promising Approach to Target Biofilm Associated Infections. *Molecules* **2022**, *27* (3), 758.

(5) Ivanova, E. P.; Hasan, J.; Webb, H. K.; Truong, V. K.; Watson, G. S.; Watson, J. A.; Baulin, V. K.; Pogodin, S.; Wang, J. Y.; Tobin, M.

J.; Lobbe, C.; Crawford, R. J. Natural Bactericidal Surfaces: Mechanical Rupture of *Pseudomonas aeruginosa* Cells by Cicada Wings. *Small* **2012**, *8* (16), 2489−2494.
(6) Fujimoto, K.; Saito, A.; Kotsuchibashi, Y. Cicada-Wing-Inspired Nanopillar Hydrogels Consisting of Poly(vinyl alcohol) and Poly(methacrylic acid) for Capturing Bacteria through Their Flexibility and Wide Range of Motion. *ACS Macro Lett.* **2022**, *11* (6), 727−732.
(7) Linklater, D. P.; Baulin, V. A.; Juodkazis, S.; Crawford, R. J.; Stoodley, P.; Ivanova, E. P. Mechano-bactericidal Actions of Nanostructured Surfaces. *Nat. Rev. Microbiol.* **2021**, *19*, 8−22.
(8) Jenkins, J.; Mantell, J.; Neal, C.; Gholinia, A.; Verkade, P.; Nobbs, A. H.; Su, B. Antibacterial Effects of Nanopillar Surfaces Are Mediated by Cell Impedance, Penetration and Induction of Oxidative Stress. *Nat. Commun.* **2020**, *11* (1), 1626.
(9) Tan, R.; Marzolini, N.; Jiang, P.; Jang, Y. Bio-inspired Polymer Thin Films with Non-close-packed Nanopillars for Enhanced Bactericidal and Antireflective Properties. *ACS Appl. Polym. Mater.* **2020**, *2* (12), 5808−5816.
(10) Ivanova, E. P.; Hasan, J.; Webb, H. K.; Gervinskas, G.; Juodkazis, S.; Troung, V. K.; Wu, A. H. F.; Lamb, R. N.; Baulin, V. A.; Watson, G. S.; Watson, J. A.; Mainwaring, D. E.; Crawford, R. J. Bactericidal Activity of Black Silicon. *Nat. Commun.* **2013**, *4*, 2838.
(11) Linklater, D. P.; De Volder, M.; Baulin, V. A.; Werner, M.; Jessl, S.; Golozar, M.; Maggini, L.; Rubanov, S.; Hanssen, E.; Juodkazis, S.; Ivanova, E. P. High Aspect Ratio Nanostructures Kill Bacteria via Storage and Release of Mechanical Energy. *ACS Nano* **2018**, *12* (7), 6657−6667.
(12) Patil, D.; Overland, M.; Stoller, M.; Chatterjee, K. Bioinspired Nanostructured Bactericidal Surfaces. *Curr. Opin. Chem. Eng.* **2021**, *34*, 100741.
(13) Roy, A.; Chatterjee, K. Bactericidal Anisotropic Nanostructures on Titanium Fabricated by Maskless Dry Etching. *ACS Appl. Nano Mater.* **2022**, *5* (3), 4447−4461.
(14) Sunline Supply Home Page. https://sunlinesupply.com/blog/how-are-nitrile-gloves-made/ (accessed 2022−09−28).
(15) Spengler, C.; Nolle, F.; Mischo, J.; Faidt, T.; Grandthyll, S.; Thewes, N.; Koch, M.; Müller, F.; Bischoff, M.; Klatt, M. A.; Jacobs, K. Strength of Bacterial Adhesion on Nanostructured Surfaces Quantified by Substrate Morphometry. *Nanoscale* **2019**, *11* (42), 19713−19722.
(16) Thewes, N.; Thewes, A.; Loskill, P.; Peisker, H.; Bischoff, M.; Herrmann, M.; Santen, L.; Jacobs, K. Stochastic binding of Staphylococcus aureus to hydrophobic surfaces. *Soft Matter* **2015**, *11* (46), 8913−8919.
(17) Primc, G.; Mozetič, M. Hydrophobic Recovery of Plasma-Hydrophilized Polyethylene Terephthalate Polymers. *Polymers* **2022**, *14* (12), 2496.
(18) Tsougeni, K.; Vourdas, N.; Tserepi, A.; Gogolides, E.; Cardinaud, C. Mechanisms of Oxygen Plasma Nanotexturing of Organic Polymer Surfaces: from Stable Super Hydrophilic to Super hydrophobic Surfaces. *Langmuir* **2009**, *25* (19), 11748−11759.
(19) Michalska, M.; Divan, R.; Noirot, P.; Laible, P. D. Antimicrobial Properties of Nanostructured Surfaces−Demonstrating the Need for a Standard Testing Methodology. *Nanoscale* **2021**, *13* (41), 17603−17614.
(20) Hasan, J.; Jain, S.; Chatterjee, K. Nanoscale Topography on Black Titanium Imparts Multi-biofunctional Properties for Orthopedic Applications. *Sci. Rep.* **2017**, *7*, 41118.
(21) Patil, D.; Sharma, A.; Aravindan, S.; Rao, P. V. Development of Hot Embossing Setup and Fabrication of Ordered Nanostructures on Large Area of Polymer Surface for Antibiofouling Application. *Micro Nano Lett.* **2019**, *14* (2), 191−195.
(22) Hasan, J.; Jain, S.; Padmarajan, R.; Purighalla, S.; Sambandamurthy, V. K.; Chatterjee, K. Multi-scale Surface Topography to Minimize Adherence and Viability of Nosocomial Drug-Resistant Bacteria. *Mater. Des.* **2018**, *140*, 332−344.
(23) Borcia, C.; Punga, I.; Borcia, G. Surface Properties and Hydrophobic Recovery of olymers Treated by Atmospheric-Pressure Plasma. *Appl. Surf. Sci.* **2014**, *317*, 103−110.
(24) Deng, C. H.; Qiao, X. Y.; Yan, Y. N.; Wang, F.; Fan, J.; Zeng, H.; Xu, X. CoPt Antidot Arrays Fabricated With Dry-Etching Using AAO Templates. *IEEE Trans. Magn.* **2016**, *52* (4), 1−5.
(25) Yabagi, J. A.; Kimpa, M. I.; Muhammad, M. N.; Nayan, N.; Embong, Z.; Agam, M. A. Nanofabrication Process by Reactive Ion Etching of Polystyrene Nanosphere on Silicon Surface. *J. Sci. Technol.* **2017**, *9* (3), 145−153.
(26) Shi, Z.; Jefimovs, K.; Romano, L.; Stampanoni, M. Towards the Fabrication of High-Aspect-Ratio Silicon Gratings by Deep Reactive Ion Etching. *Micromachines* **2020**, *11*, 864.
(27) Hong, S. H.; Hwang, J.; Lee, H. Replication of Cicada Wing's Nano-Patterns by Hot Embossing and UV Nanoimprinting. *Nanotechnology* **2009**, *20* (38), 385303.
(28) Sjöström, T.; Nobbs, A. H.; Su, B. Bactericidal Nanospike Surfaces via Thermal Oxidation of Ti Alloy Substrates. *Mater. Lett.* **2016**, *167*, 22−26.
(29) Patil, D.; Wasson, M. K.; Perumal, V.; Aravindan, S.; Rao, P. V. Bactericidal Nanostructured Titanium Surface Through Thermal Annealing. In Shunmugam, M., Kanthababu, M., Eds.; *Advances in Micro and Nano Manufacturing and Surface Engineering*; Springer: Singapore, 2019. DOI: 10.1007/978-981-32-9425-7_7.
(30) Pogodin, S.; Hasan, J.; Baulin, V. A.; Webb, H. K.; Truong, V. K.; Nguyen, T. H. P.; Boshkovikj, V.; Fluke, C. J.; Watson, G. S.; Watson, J. A.; Crawford, R. J.; Ivanova, E. P. Biophysical Model of Bacterial Cell Interactions with Nanopatterned Cicada Wing Surfaces. *Biophys. J.* **2013**, *104* (4), 835−840.
(31) Watson, G. S.; Green, D. W.; Watson, J. A.; Zhou, Z.; Li, X.; Cheung, G. S. P.; Gellender, M. A Simple Model for Binding and Rupture of Bacterial Cells on Nanopillar Surfaces. *Adv. Mater. Inter.* **2019**, *6* (10), 1801646.
(32) Xiao, K.; Cao, X.; Chen, X.; Hu, H.; Wu, C. Bactericidal Efficacy of Nanopatterned Surface Tuned by Topography. *J. Appl. Phys.* **2020**, *128*, 064701.
(33) Arnoldi, M.; Fritz, M.; Bäuerlein, E.; Radmacher, M.; Sackmann, E.; Boulbitch, A. Bacterial Turgor Pressure Can Be Measured by Atomic Force Microscopy. *Phys. Rev. E* **2000**, *62* (1), 1034−1044.
(34) Deng, Y.; Sun, M.; Shaevitz, J. W. Measuring Peptidoglycan Elasticity and Stress-Stiffening of Live Bacterial Cells. *Biophys. J.* **2011**, *100*, 514−515.
(35) Xue, F.; Liu, J.; Guo, L.; Zhang, L.; Li, Q. Theoretical Study on the Bactericidal Nature of Nanopatterned Surfaces. *J. Theor. Biol.* **2015**, *385*, 1−7.
(36) Li, X. Bactericidal Mechanism of Nanopatterned Surfaces. *Phys. Chem. Chem. Phys.* **2016**, *18*, 1311−1316.
(37) Truong, V. K.; Geeganagamage, N. M.; Baulin, V. A.; Vongsvivut, J.; Tobin, M. J.; Luque, P.; Crawford, R. J.; Ivanova, E. P. The Susceptibility of Staphylococcus Aureus CIP 65.8 And Pseudomonas Aeruginosa ATCC 9721 Cells to the Bactericidal Action of Nanostructured Calopteryx Haemorrhoidalis Damselfly Wing Surfaces. *Appl. Microbiol. Biotechnol.* **2017**, *101*, 4683−4690.

https://doi.org/10.1021/acsmacrolett.2c00697
ACS Macro Lett. 2023, 12, 227−233